KRN633: A selective inhibitor of vascular endothelial growth factor receptor-2 tyrosine kinase that suppresses tumor angiogenesis and growth

Kazuhide Nakamura,[1] Atsushi Yamamoto,[1] Masaru Kamishohara,[1] Kazumi Takahashi,[1] Eri Taguchi,[1] Toru Miura,[1] Kazuo Kubo,[1] Masabumi Shibuya,[2] and Toshiyuki Isoe[1]

[1]Pharmaceutical Development Laboratories, Kirin Brewery Co. Ltd., Takasaki, Gunma and [2]Division of Genetics, Institute of Medical Science, University of Tokyo, Tokyo, Japan

Abstract

Vascular endothelial growth factor (VEGF) and its receptor VEGFR-2 play a central role in angiogenesis, which is necessary for solid tumors to expand and metastasize. Specific inhibitors of VEGFR-2 tyrosine kinase are therefore thought to be useful for treating cancer. We showed that the quinazoline urea derivative KRN633 inhibited tyrosine phosphorylation of VEGFR-2 (IC_{50} = 1.16 nmol/L) in human umbilical vein endothelial cells. Selectivity profiling with recombinant tyrosine kinases showed that KRN633 was highly selective for VEGFR-1, -2, and -3. KRN633 also blocked the activation of mitogen-activated protein kinases by VEGF, along with human umbilical vein endothelial cell proliferation and tube formation. The propagation of various cancer cell lines *in vitro* was not inhibited by KRN633. However, p.o. administration of KRN633 inhibited tumor growth in several *in vivo* tumor xenograft models with diverse tissue origins, including lung, colon, and prostate, in athymic mice and rats. KRN633 also caused the regression of some well-established tumors and those that had regrown after the cessation of treatment. In these models, the trough serum concentration of KRN633 had a more significant effect than the maximum serum concentration on antitumor activity. KRN633 was well tolerated and had no significant effects on body weight or the general health of the animals. Histologic analysis of tumor xenografts treated with KRN633 revealed a reduction in the number of endothelial cells in non-necrotic areas and a decrease in vascular permeability. These data suggest that KRN633 might be useful in the treatment of solid tumors and other diseases that depend on pathologic angiogenesis. [Mol Cancer Ther 2004;3(12):1639–49]

Introduction

The formation of new blood vessels (angiogenesis) is essential for tumor progression and metastasis (1). This process is strictly controlled by positive angiogenic factors and negative regulators; therefore, tumors without an angiogenic phenotype cannot grow beyond a certain size and remain in a state of dormancy. However, once tumors become capable of angiogenesis due to somatic mutations that alter the balance between angiogenic factors and negative regulators, they can grow rapidly and metastasize (2).

Vascular endothelial growth factor (VEGF) is the angiogenic factor that is most closely associated with aggressive disease in numerous solid tumors. Overexpression of VEGF by tumor cells frequently occurs in response to hypoxia (3, 4), loss of tumor suppressor gene function (5, 6), and oncogene activation (7). Elevated VEGF levels are correlated with increased microvessel counts and poor prognosis in many human cancers (8–10). This correlation is attributed to the ability of VEGF to stimulate endothelial cell proliferation, protease expression, cell migration, and the formation of capillary tubes (11–13). Furthermore, VEGF functions as a potent prosurvival (antiapoptotic) factor for endothelial cells in newly formed blood vessels (14–16). In addition to the effects on preexisting vessels, VEGF also influences the mobilization and differentiation of bone marrow–derived endothelial cell progenitors that can contribute to the formation of new blood vessels (17, 18).

The receptor tyrosine kinase (RTK) VEGF receptor (VEGFR)-2 is almost exclusively located on endothelial cells (19). Its expression levels are low in normal tissues and only increase in pathologic states when neovascularization occurs. VEGFR-2 has an extracellular VEGF-binding domain, a single membrane-spanning domain, and an intracellular split tyrosine kinase domain. Binding of VEGF and VEGFR-2 induces receptor tyrosine phosphorylation and stimulates the phospholipase Cγ-protein kinase C-mitogen-activated protein (MAP) kinase/extracellular signal-regulated kinase (ERK) pathway, as well as the phosphatidylinositol 3′-kinase/AKT pathway (20, 21). VEGFR-2 is therefore thought to provide both mitogenic and survival signals and to be a major signaling component in angiogenesis. Consequently, blockade of VEGF signaling is a highly attractive therapeutic strategy. An ideal agent would be a low molecular weight compound with the ability to cross membranes, bind specifically to VEGFR-2,

Received 3/24/04; revised 8/9/04; accepted 10/18/04.

The costs of publication of this article were defrayed in part by the payment of page charges. This article must therefore be hereby marked advertisement in accordance with 18 U.S.C. Section 1734 solely to indicate this fact.

Requests for reprints: Kazuhide Nakamura, Pharmaceutical Development Laboratories, Kirin Brewery Co. Ltd., 3 Miyahara, Takasaki, Gunma 370-1295, Japan. Phone: 81-27-346-9423; Fax: 81-27-347-5280. E-mail: ka-nakamura@kirin.co.jp

Copyright © 2004 American Association for Cancer Research.

Downloaded from mct.aacrjournals.org on April 10, 2021. © 2004 American Association for Cancer Research.

and inhibit its tyrosine kinase. Such a compound should be effective when administered p.o. because it is likely that continuous blockade of the VEGF pathway would be required to control tumor growth.

In this study, we describe a novel quinazoline urea derivative, KRN633, which strongly and selectively inhibits VEGFR-2 tyrosine kinase and intracellular VEGF signaling. We also report the effect of the p.o. administration of KRN633 on the *in vivo* growth of human tumor xenografts in mice and rats.

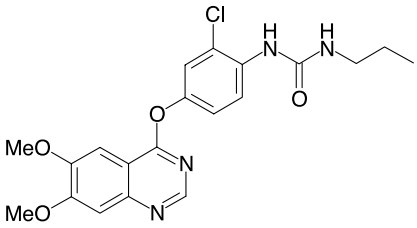

Figure 1. Chemical structure of KRN633.

Materials and Methods

KRN633

KRN633 was synthesized in the Production Department of the Research and Development Center of the Kirin Brewery Co., Ltd. (Tokyo, Japan). The chemical name of this compound is *N*-{2-chloro-4-[(6,7-dimethoxy-4-quinazolinyl)oxy] phenyl}-*N*′-propylurea and its chemical structure is shown in Fig. 1. For the *in vitro* studies, KRN633 was dissolved in DMSO and diluted in growth medium immediately before use; the DMSO concentration was 0.1% in all *in vitro* assays. For the *in vivo* studies, KRN633 was suspended in vehicle (0.5% methylcellulose in distilled water) and given to mice or rats within 1 day of its preparation.

Cells

Human umbilical vein endothelial cells (HUVEC) and normal human dermal fibroblasts were obtained from Cambrex (Walkersville, MD). VEGFR-1-overexpressing NIH3T3 cells, designated as NIH3T3-Flt-1 cells, have been previously described (22). Human chronic myelogenous leukemia cells (Ku812-F) were obtained from the Cell Resource Center for Biomedical Research of Tohoku University (Sendai, Japan). The human epidermoid carcinoma (A431) cell line was obtained from the Health Science Research Resources Bank (Osaka, Japan). Human lung carcinoma (Calu-6), human colon carcinoma (HT29, Ls174T, and SW620) and human prostate carcinoma (Du145, LNCap, and PC-3) cell lines were purchased from the American Type Culture Collection (Manassas, VA). The human lung carcinoma (A549) cell line was obtained from the Institute of Physical and Chemical Research (Tsukuba, Japan). Finally, the human lung squamous cell carcinoma (LC-6-JCK) cell line was obtained as a tumor fragment from the Central Institute for Experimental Animals (Kawasaki, Japan).

Cell-Free and Cellular Kinase Assays

Cell-free kinase assays were done to obtain IC_{50} values against a variety of recombinant receptor and non-RTKs. KRN633 was tested from 0.3 nmol/L to 10 μmol/L. All assays were done in quadruplicate with 1 μmol/L ATP.

For the cellular assays, the cells were cultured in the following media: EGM-2 (Cambrex) for the HUVECs; DMEM (Sigma-Aldrich, St. Louis, MO) containing 10% fetal bovine serum (FBS) and 200 μg/mL Geneticin (G418) for the NIH3T3-Flt-1 cells; RPMI 1640 (Sigma-Aldrich) containing 10% FBS for the Ku812-F cells; FGM-2 (Cambrex) for the normal human dermal fibroblasts; and DMEM containing 10% FBS for the A431 cells. All cells were serum starved for 16 to 24 hours in their respective basal media with 0.5% FBS. KRN633 was then added to the cells and they were incubated for 1 hour. The cells were stimulated with 50 ng/mL VEGF, 100 ng/mL stem cell factor, 50 ng/mL platelet-derived growth factor (PDGF)-BB, 20 ng/mL epidermal growth factor (PeproTech EC Ltd, London, United Kingdom), 25 ng/mL basic fibroblast growth factor (bFGF, Upstate Biotechnology, Inc., Lake Placid, NY), or 50 ng/mL hepatocyte growth factor/scatter factor (BD Biosciences Discovery Labware, Bedford, MA) at 37°C. Receptor phosphorylation was induced for 5 minutes, except for c-Kit and c-Met, which were induced for 15 and 10 minutes, respectively.

Cells were lysed with lysis buffer (1% NP40, 0.5% sodium deoxycholate, 0.1% SDS, 100 μg/mL phenylmethylsulfonyl fluoride, 1 mmol/L Na_3VO_4, and 3% aprotinin in PBS). The receptors were immunoprecipitated, subjected to SDS-PAGE, and transferred to polyvinylidene fluoride microporous membranes. All antibodies for immunoprecipitation were obtained from Santa Cruz Biotechnology, Inc. (Santa Cruz, CA). The membranes were probed with phosphotyrosine antibody 4G10 (Upstate Biotechnology). Phosphorylation was detected with peroxidase-conjugated anti–immunoglobulin G and enhanced chemiluminescence reagent (Amersham Biosciences Inc., Piscataway, NJ). Blots of the receptors were scanned and the density was quantified using the public domain software package Scion Image Beta 4.02 for Windows (Scion Corporation, Frederick, MD). IC_{50} values were calculated by nonlinear regression analysis using GraphPad Prism (GraphPad Software, Inc., San Diego, CA).

MAP Kinase Activation

After serum starvation (0.5% FBS), HUVECs were incubated with KRN633 for 1 hour and stimulated with either 50 ng/mL VEGF or 25 ng/mL bFGF. Cell lysates were subjected to SDS-PAGE. Immunoblotting of phosphorylated MAP kinases was done using phospho-p44/42 MAP kinase antibody (Cell Signaling Technology Inc., Beverly, MA).

Endothelial Cell Proliferation

Endothelial cell-proliferation assays were done as described previously (23). Briefly, HUVECs were seeded in collagen-coated 96-well plates at 4,000 cells per 200 μL/well in M-199 (Invitrogen Corp., Carlsbad, CA) containing 5% FBS. After 24 hours, KRN633 was added followed by

Downloaded from mct.aacrjournals.org on April 10, 2021. © 2004 American Association for Cancer Research.

20 ng/mL VEGF or 10 ng/mL bFGF, and the cells were cultured for 78 hours. [^{3}H]thymidine (1 μCi/mL) was added and the cells were cultured for a further 14 hours. They were then harvested and their radioactivity was measured using a liquid scintillation counter (Wallac 1205 Beta Plate; Perkin-Elmer Life Sciences, Boston, MA).

Capillary Tube Formation

Capillary tube formation of endothelial cells was measured by coculture with normal human dermal fibroblasts. Normal human dermal fibroblasts in FGM-2 were plated in 24-well plates at 5×10^4 cells/well and cultured for 24 hours. HUVECs were then added at 3,000 cells/well. After 24 hours, KRN633 was added followed by 10 ng/mL VEGF. The cells were cocultured for 9 days, fixed in ice-cold 70% ethanol for 30 minutes, and the HUVECs visualized by immunocytochemical detection of von Willebrand factor (TCS Biologicals Ltd., Buckingham, United Kingdom). The areas, lengths, paths, and joints of the stained tubelike structures were measured using an angiogenesis image analyzer (Kurabo, Osaka, Japan) in five different fields for each condition.

Cytotoxicity Assays

Cancer cells were plated in media with 10% FBS and antibiotics, at densities known to permit exponential growth over the assay period. The details were as follows: A549 in DMEM at 200 cells/well; Ls174T and DU145 in Eagle's MEM (Invitrogen) with 2 mmol/L L-glutamine (Invitrogen) at 3,000 cells/well; HT29 in McCoy's 5a (Invitrogen) at 3,000 cells/well; LNCap in RPMI 1640 (Sigma-Aldrich) at 3,000 cells/well; and PC-3 in Ham's F12K medium (Invitrogen) with 2 mmol/L L-glutamine at 3,000 cells/well. The cells were cultured for 24 hours before adding KRN633 (0.01 to 10 μmol/L) or vehicle (0.1% DMSO in medium) and then grown for a further 96 hours. Cell viability was measured using WST-1 reagent (Roche Applied Science, Indianapolis, IN). The percentage viability was determined relative to the untreated control.

Tumor-Xenograft Models

All *in vivo* experiments were conducted in accordance with the guidelines of the Kirin Animal Care and Use Committee. Athymic mice (BALB/cA, Jcl-nu) and athymic rats (F344/N, Jcl-rnu) were obtained from CLEA Japan Inc. (Tokyo, Japan). Mice and rats were housed in a barrier facility with a 12-hour light/dark cycle, and provided with sterilized food and water *ad libitum*.

A549, Ls174T, HT29, DU145, LNCap, and PC-3 cells were cultured in the appropriate media and implanted s.c. into the hind flanks of mice or rats. To facilitate tumor grafting, DU145, LNCap, and PC-3 were suspended in Matrigel (BD Biosciences Discovery Labware) and diluted 1:1 in the relevant medium before implantation. LC-6-JCK tumor xenografts were established in the hind flank by s.c. implantation of a cubic tumor fragment of ~2-mm diameter. Mice were grouped randomly when the tumors had reached an average volume of 100 to 260 mm^3 for standard models (day 0) and 500 to 670 mm^3 for well-established models. Rats were grouped randomly when tumors had reached an average volume of 162 to 618 mm^3. The animals were then given KRN633 by p.o. gavage (as described in the figure and table legends). Tumor volume was measured twice weekly using Vernier calipers and was calculated as length × width × height × 0.5. Relative tumor volume (RTV) was calculated using the following formula: RTV at day X = (tumor volume at day X)/(tumor volume at day 0). Percentage tumor growth inhibition (TGI%) was calculated as follows: TGI% at day X = [(RTV of vehicle-treated group at day X − RTV of KRN633-treated group at day X)/(RTV of vehicle-treated group at day X − 1)] × 100. P values were determined by comparing mean tumor size in the treated group with mean tumor size in the vehicle-treated group using Dunnett's test.

Immunohistochemistry

A549 tumor xenografts were established in athymic rats as described above. Drug treatments were initiated when the tumor volumes were ~440 mm^3. Rats received KRN633 (as described in the figure and table legends). Tumor tissues were harvested and cryosections of ~4 μm were prepared. Immunofluorescence staining was done using biotinylated anti-rat CD31 antibody (BD Biosciences PharMingen, San Diego, CA) and TSA fluorescence systems (Perkin-Elmer Life Sciences). To identify viable regions of the tumor, each serial section was stained with H&E. The areas of CD31$^+$ endothelial cells within the viable regions were measured by imaging sections digitally and processing five random 0.2122-mm^2 fields per slide at ×200 magnification with LSM510 systems (Version 2.01; Carl Zeiss MicroImaging, Inc., Thornwood, NY).

Tumor Vascular Permeability Assays

Tumor blood vessel leakage was determined using the Evans Blue dye perfusion technique (24) with some modifications. Rats with A549 tumor xenografts were i.v. injected with 12.5 mL/kg of Evans Blue dye solution (10 mg/mL). After 30 minutes, they were sacrificed and the A549 tumors were harvested immediately. Dye was extracted from the tumors and measured spectrophotometrically.

Determination of Serum Concentrations after Oral Administration

At the allotted times, blood samples were collected from the heart or tail vein of athymic mice and rats, respectively. Serum samples were analyzed by reverse phase high-performance liquid chromatography (HPLC) using the tandem mass spectrometry method. Briefly, KRN633 and internal standard were extracted from serum samples using methyl-*t*-butylether. The organic phase was evaporated to dryness, reconstituted with the mobile phase, and then analyzed directly. KRN633 concentrations were determined from the peak area ratio of KRN633 and internal standard. The quantification range was 0.4 to 200 ng/mL.

Pharmacokinetic Analysis

Serum concentration-time data were analyzed by a non-compartmental pharmacokinetic method using WinNonlin version 2.1 (Pharsight Corporation, Mountain View, CA) to determine the area under the serum concentration-time curve extrapolated to infinity (AUC_∞), the apparent terminal-elimination half-life ($t_{1/2}$), oral clearance (CL/F), and the apparent distribution volume (Vd/F). The maximum serum

Downloaded from mct.aacrjournals.org on April 10, 2021. © 2004 American Association for Cancer Research.

concentration (C_{max}) and the time at which C_{max} was achieved (T_{max}) were obtained directly from the serum concentration data. The serum concentration-time profiles after repeated administration were simulated by WinNonlin using the pharmacokinetic parameters obtained from compartment-model analysis of the profile after single p.o. administration at a dose of 20 mg/kg.

Results

Effects of KRN633 on RTKs

The inhibitory effects of KRN633 on various RTKs in both cell-free and cellular assays were evaluated. In cell-free assays, using 1 μmol/L ATP, KRN633 strongly inhibited VEGFR-1, -2 and -3 (IC_{50} = 170, 160, and 125 nmol/L, respectively). It also weakly inhibited PDGF receptor (PDGFR)-α and -β, c-Kit, breast tumor kinase, and tunica interna endothelial cell kinase tyrosine kinases (IC_{50} = 965, 9,850, 4,330, 9,200, and 9,900 nmol/L, respectively). The IC_{50} values for EGFR, EphB2 and -B4, insulin-like growth factor-1 receptor, fibroblast growth factor receptor (FGFR)-1, -3 and -4, Abl, erbB4, fme-like tyrosine kinase-3, insulin receptor, Janus kinase 2, c-Met, muscle-specific RTK, Wee1, Src, and focal adhesion kinase tyrosine kinases were all >10 μmol/L.

The cellular assays used the appropriate normal and cancer cell lines, and phosphorylation of the RTKs was stimulated with their cognate ligands. The effect of KRN633 was measured by immunoblotting with antiphosphotyrosine antibody after immunoprecipitation. As shown in Table 1, the phosphorylation of VEGFR-2 was potently inhibited by exposure to KRN633 for 1 hour prior to stimulation with VEGF (IC_{50} = 1.16 nmol/L). KRN633 also inhibited the phosphorylation of VEGFR-1 (IC_{50} = 11.7 nmol/L), c-Kit, and PDGFR-β (IC_{50} = 8.01 and 130 nmol/L, respectively), both of which contain a large insert within the kinase domain. KRN633 did not block the phosphorylation of FGFR-1, EGFR, or c-Met, even at a concentration of 10 μmol/L.

Table 1. Effects of KRN633 on the ligand-stimulated phosphorylation of RTKs

RTK	Cell	IC_{50} (nmol/L)	95% Confidence intervals (nmol/L)	Fold selectivity*
VEGFR-2	HUVEC	1.16	0.88-1.53	1.00
VEGFR-1	NIH3T3-Flt-1†	11.7	6.7-20.4	10.1
c-Kit	KU812F	8.01	6.3-10.3	6.90
PDGFR-β	NHDF	130	103-164	112
FGFR-1	NHDF	>10,000		>8,600
EGFR	A431	>10,000		>8,600
c-Met	A431	>10,000		>8,600

NOTE: Serum-starved cells were treated with or without KRN633 for 1 hour before the stimulation of cognate ligands. After stimulation, receptors in the cell lysates were immunoprecipitated with the antireceptor antibody and immunoblotted with an antiphosphotyrosine monoclonal antibody (see Materials and Methods section for further details). All assays were done in quadruplicate (n = 4). IC_{50} values and their 95% confidence intervals were calculated by nonlinear regression analysis of the percentage inhibition. *NHDF,* normal human dermal fibroblast.
*Ratio for the IC_{50} obtained with a given RTK compared to that achieved versus VEGFR-2.
† flt-1-transfected NIH3T3.

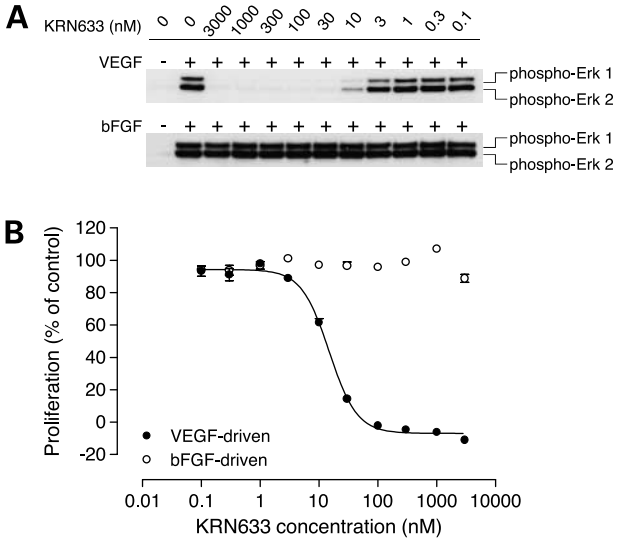

Figure 2. Effects of KRN633 on the VEGF-induced MAP kinase activation and proliferation of endothelial cells. **A,** KRN633 blocked MAP kinase activation induced by VEGF, but not that induced by bFGF. Serum-starved HUVECs were treated with KRN633 for 1 hour before stimulation with either VEGF (*top*) or bFGF (*bottom*). After lysis, the cell lysates were subjected to SDS-PAGE and immunoblotting with anti–phospho-ERK1/2 antibody. **B,** KRN633 inhibited VEGF-driven HUVEC proliferation but not bFGF-driven proliferation. HUVECs were seeded and cultured for 24 hours. Cells were incubated with KRN633 before stimulation with 20 ng/mL VEGF (●) or 10 ng/mL bFGF (○). The cells were then cultured for 78 hours followed by incubation with [^{3}H]thymidine (1 μCi/mL) for 14 hours. The incorporated radioactivity of the cells was measured using a liquid scintillation counter. *Points,* means (n = 12); *bars,* SE.

KRN633 Inhibits VEGF-Dependent MAP Kinase Phosphorylation and Endothelial Cell Proliferation

Although VEGF activates several signaling pathways via VEGFR-2 in endothelial cells, MAP kinase is of major importance in the induction of endothelial cell proliferation by VEGF, bFGF, and EGF (25). We therefore investigated the effect of KRN633 on the phosphorylation of MAP kinases (ERK1 and -2) in response to VEGF and bFGF by immunoblotting with anti–phospho-ERK1/2 antibody. KRN633 inhibited VEGF-dependent phosphorylation of the MAP kinases (Fig. 2A); the IC_{50} values for ERK1 and -2 were 3.51 and 6.08 nmol/L, respectively. By contrast, KRN633 did not reduce the bFGF-dependent phosphorylation of MAP kinases, even at a concentration of 3 μmol/L.

KRN633 also inhibited the VEGF-driven proliferation of HUVECs, as assessed using a [^{3}H]thymidine incorporation assay (IC_{50} = 14.9 nmol/L; Fig. 2B). However, FGF-driven proliferation was only weakly inhibited at 3 μmol/L. These results are consistent with the ability of KRN633 to reduce

Downloaded from mct.aacrjournals.org on April 10, 2021. © 2004 American Association for Cancer Research.

the VEGF-induced phosphorylation of VEGFR-2, but not the bFGF-induced phosphorylation of FGFR-1. Our findings suggest that KRN633 blocks VEGF signaling by inhibiting VEGFR-2 phosphorylation in endothelial cells.

KRN633 Suppresses Capillary Tube Formation of Endothelial Cells *In vitro*

To investigate the effect of KRN633 on *in vitro* tube formation by endothelial cells, HUVECs were cocultured with fibroblasts in the presence of KRN633. The formation of capillary-like structures induced by 10 ng/mL VEGF was inhibited by KRN633 (Fig. 3A). The average area of the tubes, cell overcrowding, total length of the tubes, and number of capillary connections and paths per field were measured (Fig. 3B). There was limited formation of capillary-like structures without VEGF stimulation. VEGF increased the average area, total tube length, number of capillary connections, and number of paths per field by 2.9-, 3.4-, 39-, and 7.4-fold, respectively. KRN633 at a concentration of 3 nmol/L approximately halved the increase in the number of capillary connections and paths. At a concentration of 10 nmol/L, it also inhibited the increase in average area and total tube length by ~50%. At a concentration of 30 nmol/L or more, the parameters of tube formation were reduced to below their basal levels. These findings suggest that KRN633 can block survival signaling by VEGF and trigger the apoptosis of HUVECs at sufficiently high concentrations.

Effects of KRN633 on Tumor Growth *In vivo*

The antitumor action of KRN633 against a variety of human tumors was investigated in athymic mouse xenograft models. Representative results are summarized in Table 2. In standard xenograft models (initial tumor volume, 103–260 mm^3), once-daily administration of KRN633 produced >50% tumor growth inhibition in LC-6-LCK, HT29, Ls174T, and LNCap cells, and slight regression of A549 tumors at 100 mg/kg/d (Table 2A). It also caused marked inhibition of the growth of Du145 tumors (Table 2A). These data indicate that KRN633 is effective against lung, colon, and prostate tumor lines after 2 weeks of repeated p.o. administration.

The effect of KRN633 on well-established tumor xenografts (initial tumor volume, 500–667 mm^3) was also examined. Treatment with KRN633 was initiated when A549, HT29, and Du145 tumors reached an average size of ~500 to 700 mm^3. Twice-daily administration of KRN633 at 100 mg/kg induced ~90% growth inhibition of HT29 tumors and caused the regression of A549 and Du145 tumors by ~35% and 60%, respectively (Table 2B). The antitumor effect in each established tumor model was superior to that in the corresponding standard (less well established) tumor model. This suggests that the antitumor activity of KRN633 is less affected by initial tumor size. In the periodic intermittent-dosing model, the resumption of

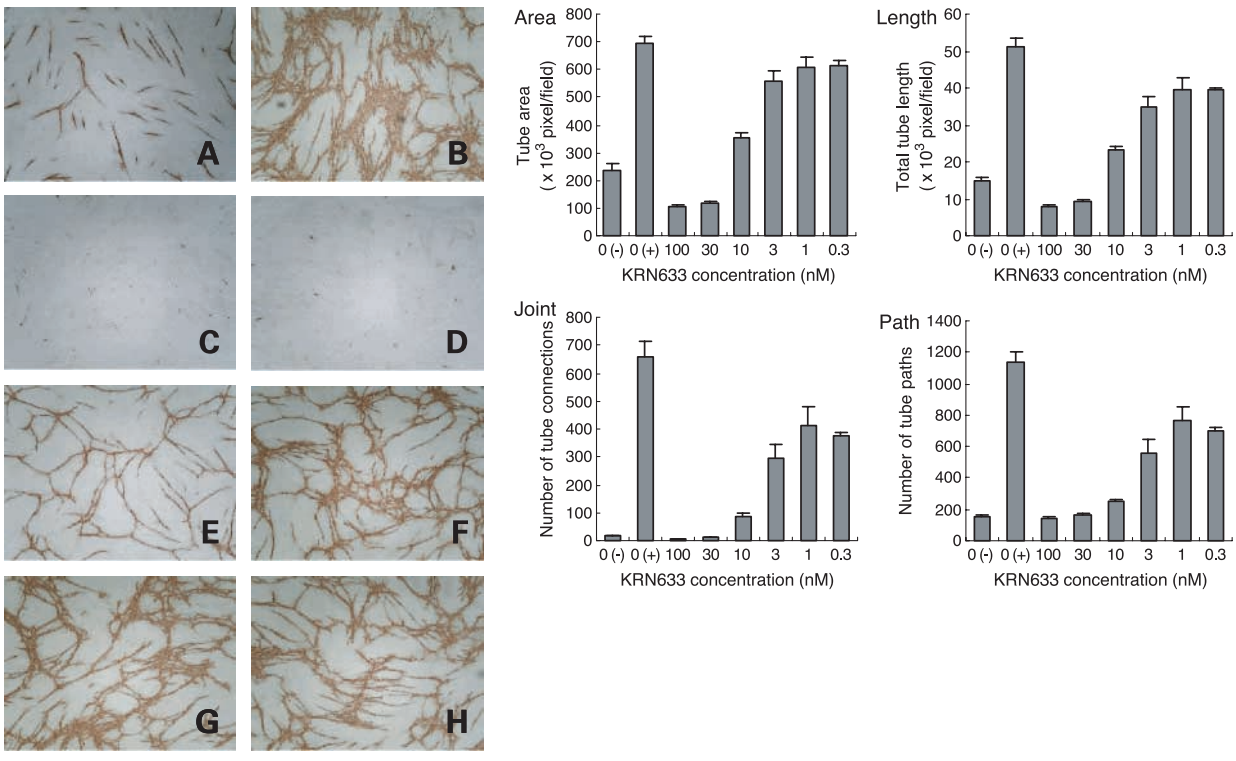

Figure 3. Effect of KRN633 on endothelial cell tube formation induced by VEGF. HUVECs were cocultured with human fibroblasts, as described in Materials and Methods. 0.1% DMSO (**A** and **B**) or KRN633 at a concentration of 100 (**C**), 30 (**D**), 10 (**E**), 3 (**F**), 1 (**G**), or 0.3 nmol/L (**H**) were added to the medium followed by stimulation with 10 ng/mL VEGF (**B**–**H**). The cells were then incubated for 9 days. The area, length, paths, and joints of the stained tubelike structures were measured quantitatively using image analysis software in five different fields for each condition. *Columns,* means ($n = 5$); *bars,* SE.

Downloaded from mct.aacrjournals.org on April 10, 2021. © 2004 American Association for Cancer Research.

Table 2. Effects of KRN633 on human tumor xenografts in athymic mice

Cell	Tissue of Origin	Initial Volume (mm^3)	Treatment	Dose (mg/kg)	TGI at day 14 (%)	Regression (%)
A. "Regular" Tumors						
A549	Lung	120	qd 2 wk	20	42.1*	
				100	>100 †	4
			bid 2 wk	10	52.3*	
				20	68.2 †	
				50	>100 †	9
				100	>100 †	13
LC6	Lung	179	qd 2 wk	100	51.5	
Calu6	Lung	122	qd 2 wk	100	34.3	
HT29	Colon	110	qd 2 wk	20	45.3	
				100	60.1	
		144	bid 2 wk	20	57.4*	
				100	76.3 †	
SW620	Colon	115	qd 2 wk	100	3.7	
Ls174T	Colon	150	qd 2 wk	20	35.7	
				100	56.4	
DU145	Prostate	103	qd 2 wk	20	71.2*	
				100	>100 †	2
		131	bid 2 wk	20	>100*	18
				100	>100 †	56
PC3	Prostate	260	qd 2 wk	100	34.5	
LNCap	Prostate	170	qd 2 wk	100	60.2 ‡	
B. "Well-established" Tumors						
A549	Lung	667	qd 2 wk	20	33.9	
				100	59.7	
			bid 2 wk	10	18.4	
				20	>100 ‡	15
				50	>100 ‡	9
				100	>100 †	35
HT29	Colon	500	qd 2 wk	20	35.3	
				100	60.4 ‡	
			bid 2 wk	10	57.9	
				20	61.5 ‡	
				50	73.8 ‡	
				100	89.8*	
DU145	Prostate	520	qd 2 wk	20	>100 ‡	29
				100	>100 †	62
		511	bid 2 wk	10	>100 †	35
				20	>100 †	36
				50	>100 †	48
				100	>100 †	63

NOTE: Human tumor xenografts were established in the hind flank of athymic mice (BALB/cA, Jcl-nu). The mice were randomized into groups of five at the point when the tumors reached the average sizes indicated: 103 to 260 mm^3 ("regular"; A) or 500 to 667 mm^3 ("well-established"; B). They were then treated with KRN633 or vehicle, either once (*qd*) or twice (*bid*) per day, at the dosages shown. The percentage of tumor growth inhibition (*TGI*) compared with the vehicle-treated group was calculated on the day after the last treatment (day 14). Tumor regression rates at day 14, relative to the tumor sizes at which the treatments were initiated, are also shown.
*$P < 0.01$.
†$P < 0.001$.
‡$P < 0.05$.

treatment led to the regression of DU145 tumors that had regrown after treatment had ceased; this indicates that tumors are less likely to acquire resistance to KRN633 (Fig. 4).

The effect of KRN633 on tumor growth was also evaluated in athymic rat xenograft models; the results are summarized in Table 3. Once-daily p.o. administration of KRN633 for 14 days inhibited tumor growth in rats as well as mice. Twice-daily administration of KRN633 had a stronger effect on A549 tumor growth than once-daily administration at the same total dose. KRN633 was well tolerated in all of the *in vivo* experiments and had no significant effects on the body weight or general health of the animals.

Downloaded from mct.aacrjournals.org on April 10, 2021. © 2004 American Association for Cancer Research.

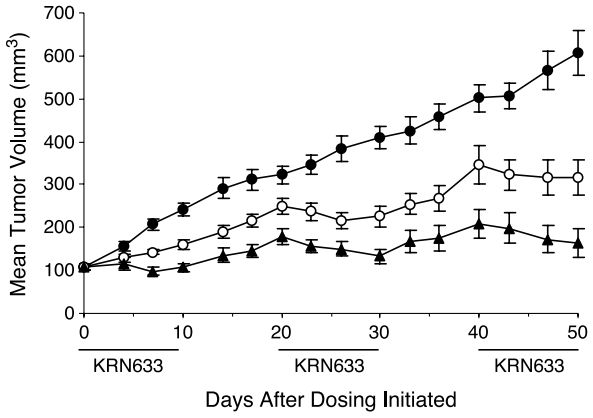

Figure 4. Effect of periodic intermittent dosing of KRN633 on the s.c. tumor growth of DU145. Once-daily p.o. administration of KRN633 at doses of 20 (○) or 100 mg/kg/d (▲), or vehicle (●), were initiated when tumors reached an average of 107 to 110 mm^3. After 10 days, the dosing was stopped to monitor tumor regrowth. KRN633 administration resumed on day 20 and was terminated on day 29. Administration recommenced on day 40 and finally ended on day 49. *Points,* mean tumor volume per group ($n = 8$); *bars*, SE.

We examined the effects of KRN633 on the *in vitro* proliferation of all tumor cells used in the *in vivo* xenograft models with the exception of LC-6-JCK, which was maintained as tumor fragments. KRN633 had no significant inhibitory action against any of the cell lines, even at a concentration of 10 mol/L; this suggests that the *in vivo* antitumor effects of KRN633 are not due to cytotoxicity (data not shown).

KRN633 Inhibits Tumor Angiogenesis and Vascular Permeability

To determine whether the inhibition of tumor growth was associated with a reduction in tumor vessel formation, we examined the histology of implanted A549 tumors in athymic rats. Treatment with 2, 10, and 50 mg/kg KRN633 twice daily p.o. for 14 days reduced the numbers of $CD31^+$ cells in viable regions of the tissue by 15%, 53%, and 76%, respectively (Fig. 5). These doses also increased the percentage of necrotic areas within the A549 tumors, and inhibited tumor growth by 58%, 95%, and >100%, respectively. These findings reflect the antitumor activity in the athymic rat xenograft models (data not shown).

The effect of KRN633 on vascular permeability was also investigated. KRN633 was given p.o. to athymic rats bearing A549 tumor xenografts. Administration of KRN633 at 2, 10, and 50 mg/kg (twice daily p.o.) for 3 days decreased the amount of Evans Blue extracted from the tumors by 16%, 49%, and 74%, respectively, indicating that KRN633 attenuates vascular permeability as well as tumor vessel formation at an early stage of treatment (Fig. 5C).

Table 3. Effects of KRN633 on human tumor xenografts in athymic rats

Cell	Tissue of Origin	Initial Volume (mm^3)	Treatment	Dose (mg/kg)	TGI at day 14 (%)	Regression (%)
A549	Lung	162	qd 2 wk	2	17.2	
				5	28	
				10	56.9	
				20	47.1	
				50	77.9*	
				100	95.4 †	
		557	bid 2 wk	1	40.1 ‡	
				2	34.7 ‡	
				5	62.5 †	
				10	87.2 †	
				20	95 †	
				50	>100 †	3
HT29	Colon	616	qd 2 wk	1	39.6	
				5	68.8 †	
				20	87.7 †	
				100	>100 †	8
DU145	Prostate	657	qd 2 wk	5	22.2	
				10	64.7 ‡	
				20	65.8 ‡	
				50	89.6*	
				100	>100 *	3

NOTE: Human tumor xenografts were established in the hind flank of athymic rats (BALB/cA, Jcl-nu). Rats were randomized into groups of five at the point when the tumors reached the average size indicated (162 to 657 mm^3) and were then treated with KRN633 or vehicle, either once (*qd*) or twice (*bid*) per day, at the dosages shown. The percentage of tumor growth inhibition compared with the vehicle-treated group was calculated on the day after the last treatment (day 14).
*$P < 0.01$.
†$P < 0.001$.
‡$P < 0.05$.

Downloaded from mct.aacrjournals.org on April 10, 2021. © 2004 American Association for Cancer Research.

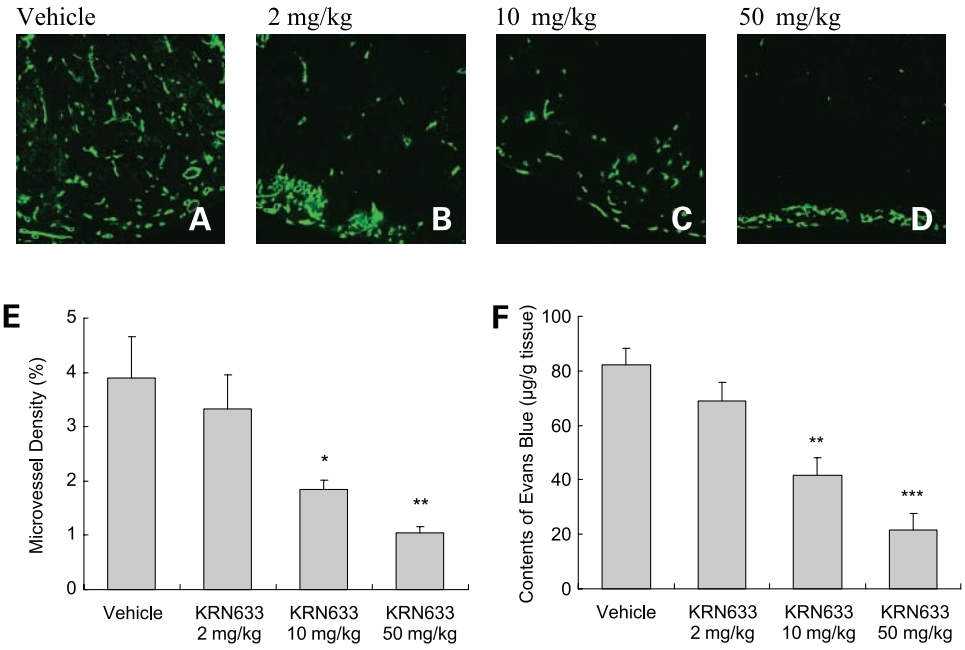

Figure 5. Effect of KRN633 on tumor microvessel density and vascular permeability. Athymic rats bearing A549 tumors were treated with KRN633 at the doses indicated or with vehicle, twice daily for 2 weeks. The tumors were then harvested. Cryosections of the tumor tissues were taken from the groups treated with vehicle (**A**) and KRN633 (**B–D**). Immunohistochemical staining for CD31 was done to visualize the blood vessels. **E,** microvessel density (percentage of $CD31^+$ area per tumor area) was determined by image analysis. *Columns,* means; *bars,* SE. *P* values were calculated by comparing the means of the treated groups and the control (vehicle) group using Dunnett's test. $*P < 0.05$; $**P < 0.01$. **F,** athymic rats bearing A549 tumors were treated with KRN633 at doses of 2, 10, and 50 mg/kg, or with vehicle, twice daily for 3 days. Rats were given i.v. injections of Evans Blue dye solution 4 hours after the last p.o. administrations. After 30 minutes, the tumors were harvested, and the dye was extracted and measured spectrophotometrically. *Columns,* means ($n = 5$); *bars*, SE. *P* values were calculated by comparing the means of the treated groups and the control (vehicle) group using Dunnett's test. $**P < 0.01$; $***P < 0.001$.

Pharmacokinetics of KRN633 after p.o. Administration to Mice and Rats

The pharmacokinetic parameters of KRN633 after single p.o. administration to athymic mice and rats are shown in Table 4. KRN633 was absorbed after p.o. administration with a T_{max} of ~4 to 5 hours in all animals. The C_{max} of mice was ~2-fold greater than that of rats, and the $t_{1/2}$ of mice was about one-third of the value in rats. The serum concentration in mice declined relatively rapidly in a monoexponential manner.

To estimate serum concentration-time profiles after repeated p.o. administration, we simulated values at KRN633 doses of 20 mg/kg at 24-hour intervals and 10 mg/kg at 12-hour intervals. The pharmacokinetic parameters Vd/F, k_a, and k_e were calculated using one-compartment model analysis as follows: 26.9 L/kg, 0.313 h^{-1}, and 0.113 h^{-1} for mice, and 8.14 L/kg, 0.344 h^{-1}, and 0.347 h^{-1} for rats, respectively. In mice, the simulated peak and trough serum concentrations at steady state (C_{max}^{ss} and C_{min}^{ss}) at intervals of 24 hours were 902 and 5.09 ng/mL, respectively; the corresponding values at intervals of 12 hours were 489 and 82.9 ng/mL (Fig. 6). In rats, the C_{max}^{ss} and C_{min}^{ss} at intervals of 24 hours were 466 and 82.4 ng/mL, respectively, and at intervals of 12 hours were 329 and 188 ng/mL, respectively (Fig. 6). In all simulations, the C_{max}^{ss} was lower and the C_{min}^{ss} was higher in rats compared with mice. In all animals,

Table 4. Pharmacokinetic parameters of KRN633 after single p.o. administration at a dose of 20 mg/kg

	T_{max} (h)	C_{max} (ng/mL)	AUC_∞ (ng h/mL)	$t_{1/2}$ (h)	CL/F (L/h/kg)	Vd/F (L/kg)
Athymic mouse	4.00 ± 0.00	899 ± 146	7800 ± 850	2.24 ± 0.03	2.58 ± 0.26	8.34 ± 0.87
Athymic rat	5.33 ± 2.31	431 ± 34	6510 ± 1360	7.60 ± 2.26	3.16 ± 0.61	33.4 ± 3.7

NOTE: Each value represents the mean ± SD. $n = 3$.

Downloaded from mct.aacrjournals.org on April 10, 2021. © 2004 American Association for Cancer Research.

multiple dosing at intervals of 12 hours led to a lower C_{max}^{ss} and a higher C_{min}^{ss} than dosing at 24-hour intervals. Furthermore, multiple dosing in rats showed a remarkable superposition effect, reflecting the relatively long $t_{1/2}$.

Discussion

Several strategies have been developed for targeting the VEGF pathway as part of anticancer therapy. Possible approaches include inhibiting the secretion of endogenous tumor VEGF; neutralizing VEGF in the microcirculation; using oligonucleotides, antibodies, and soluble VEGFRs to prevent it from binding to its receptor; and using small-molecule inhibitors of VEGF signaling in endothelial cells (26, 27). In many cases, inhibiting tumor angiogenesis by targeting VEGF signaling has been shown to induce the stasis or regression of tumor growth pathways in animal models. Moreover, the addition of Bevacizumab (a monoclonal antibody against VEGF) to fluorouracil-based combination chemotherapy has reportedly caused statistically significant and clinically meaningful improvements in survival among patients with metastatic colorectal cancer, thus reaffirming the importance of both VEGF and VEGFR (28).

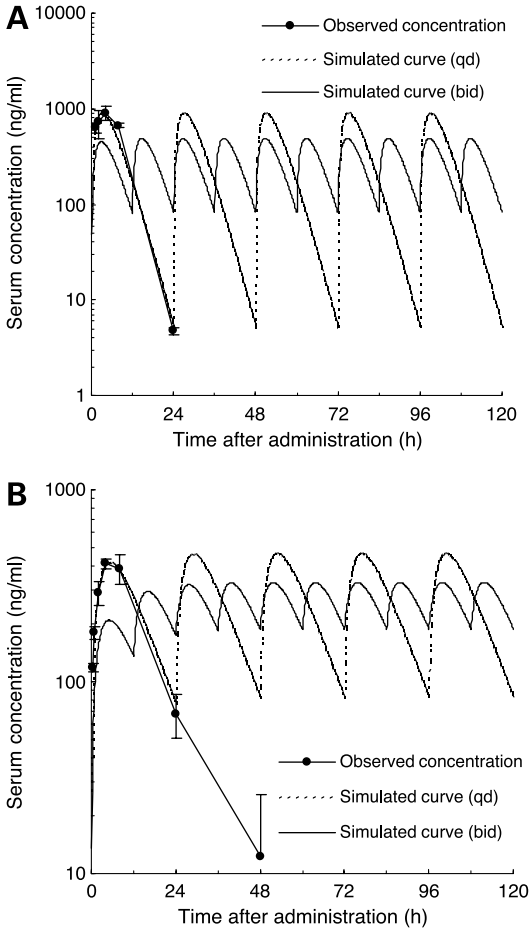

Figure 6. Simulated serum concentration-time profiles of KRN633 in athymic mice (**A**) and rats (**B**) after p.o. administration of 20 mg/kg with 24-hour intervals (*dotted line*) or 10 mg/kg with 12-hour intervals (*solid line*). *Points,* observed serum concentrations of KRN633 after single p.o. administration of a dose of 20 mg/kg (n = 3); *bars*, SD.

KRN633 is a novel quinazoline urea derivative that targets the VEGF signaling pathway in endothelial cells by inhibiting the catalytic activity of VEGFR-2 tyrosine kinase. Although our results showed that this activity was relatively weak in the cell-free assay (IC_{50} = 160 nmol/L), it was highly potent in the cellular assay (IC_{50} = 1.16 nmol/L). In comparison with other reported VEGFR inhibitors (30–34), KRN633 is a powerful inhibitor of VEGFR-2-mediated signaling in endothelial cells. KRN633 also potently inhibited the MAP kinase activation and proliferation induced by VEGF, but not by bFGF, which coincided with its selectivity for the respective RTKs. Furthermore, KRN633 inhibited tube formation by endothelial cells in an *in vitro* angiogenesis assay. There is now general agreement that VEGFR-2 is the major mediator of the mitogenic and angiogenic effects of VEGF (35). It is therefore clear that the primary mechanism by which KRN633 blocks VEGF-induced endothelial cell responses and *in vitro* angiogenesis is the inhibition of VEGFR-2 phosphorylation.

The present study found that KRN633 inhibited VEGFR-1 phosphorylation (IC_{50} = 11.7 nmol/L). Despite the higher affinity for VEGF, the VEGFR-1 tyrosine kinase is not as active as that of VEGFR-2. Gene-targeting analyses suggested that it acted as a ligand-trapping molecule in embryonic development (36, 37). However, recent reports have shown elevated levels of specific ligands of VEGFR-1, such as placental growth factor and VEGF-B, in some human cancers (38, 39). Placental growth factor–overexpressing Lewis lung carcinoma cells were reported to grow much faster in wild-type mice than in Flt-1 tyrosine kinase domain–deficient mice (40). Furthermore, placental growth factor deficiency in mice can inhibit angiogenesis in many pathologic disorders, including cancer (41). VEGFR-1 activation has been shown to cause the intermolecular transphosphorylation of VEGFR-2, as well as VEGF/placental growth factor heterodimer–activated intramolecular VEGFR cross-talk, through the formation of VEGFR-1/VEGFR-2 (42). VEGFR-1 also plays an important role in the VEGF-dependent migration of macrophages (36, 43, 44), which produce several proangiogenic cytokines and growth factors in tumors (45). Taken together, these findings suggest that VEGFR-1 is involved in pathologic angiogenesis and that the inhibition of VEGFR-1 signaling might contribute to the antiangiogenic and antitumor activities of KRN633.

VEGFR-3 tyrosine kinase is also inhibited by KRN633. VEGFR-3 was initially thought to be restricted to the lymphatic endothelium (46) and, therefore, to be of less relevance to tumor angiogenesis. However, recent data suggest that its level can be elevated in tumor blood vessels during neovascularization and that tumor VEGF-C expression correlates with lymphatic invasion, increased metastasis,

Downloaded from mct.aacrjournals.org on April 10, 2021. © 2004 American Association for Cancer Research.

and relatively poor clinical prognosis (47, 48). Hence, the KRN633-induced inhibition of VEGFR-3 tyrosine kinase and its signaling in cells could potentially impart a therapeutic benefit.

It should be noted that KRN633 exhibited modest potency versus ligand-induced PDGFR-β phosphorylation despite its high potency versus VEGFR-2 phosphorylation. According to the IC_{50} comparison in the cellular assay, KRN633 seemed to be more than 100-fold less potent against PDGFR-β than VEGFR-2. Although several VEGFR-2 tyrosine kinase inhibitors have been reported (29–34), few are likely to show such highly selectivity. This unique property of KRN633 might lead to different *in vivo* efficacy and toxicity compared with other VEGFR-2 tyrosine kinase inhibitors, although this remains to be confirmed experimentally.

Based on VEGF signaling inhibition, KRN633 was expected to prevent the formation and survival of new vessels in tumors. Accordingly, we showed a reduction in the microvessel density of A549 tumor xenografts in rats, a decrease in the number of viable regions on the periphery of tumors, and an increase in the avascular and necrotic area in the center of tumors. KRN633 also decreased the vascular permeability of tumors after only 3 days of treatment. This was probably due to the inhibition of VEGF signaling by KRN633 because VEGF functions as a potent vascular permeability factor (49). Vascular permeability and the introduction of a provisional plasma-derived matrix precede and accompany the onset of endothelial cell division and new blood vessel formation in tumors (50). Therefore, the reduction of vascular permeability might be partly responsible for the inhibition of angiogenesis by KRN633.

Taken together, our results suggest that the antitumor effects of KRN633 are secondary to its antiangiogenic action based on the inhibition of VEGFRs. KRN633 is clearly suitable for the treatment of a wide range of solid tumors; it showed *in vivo* antitumor activities against various cancer cell lines, although it did not substantially inhibit their *in vitro* proliferation. Interestingly, there were differences in the effects of KRN633 on tumor growth among cancer cell lines, including those derived from the same tissue. This suggests that there might be differences in the mechanism of angiogenesis induction and/or in the reliance on vascular supply for tumor maintenance and growth among these cell lines. Further investigation of the factors affecting susceptibility will be required not only for the design, scheduling, and monitoring of antiangiogenic therapies in clinical settings but also for interpreting the results obtained from such therapies.

Pharmacokinetic analysis revealed that KRN633 was well absorbed after p.o. administration, although the $t_{1/2}$ was relatively short in mice in particular. Higher trough serum concentrations in simulations and more potent antitumor efficacy of KRN633 were observed in rats. In addition, twice-daily administration, which increased the trough serum concentrations of KRN633 during treatment in simulations, generally resulted in more potent activity than once-daily administration of a similar dose. Therefore, the trough concentration seems to be more significant for antitumor activity than the C_{max}. We propose that a target serum concentration exists at which KRN633 can sufficiently inhibit VEGF signaling in tumors. Our findings suggest that the antitumor activity of KRN633 depends on the length of time that the serum concentration remains above this target concentration rather than on the value of C_{max}.

References

1. Folkman J. Tumor angiogenesis: therapeutic implications. N Engl J Med 1971;285:1182–6.
2. Bergers G, Benjamin LE. Tumorigenesis and the angiogenic switch. Nat Rev Cancer 2003;3:401–10.
3. Shweiki D, Itin A, Soffer D, Keshet E. Vascular endothelial growth factor induced by hypoxia may mediate hypoxia-initiated angiogenesis. Nature 1992;359:843–5.
4. Forsythe JA, Jiang BH, Iyer NV, et al. Activation of vascular endothelial growth factor gene transcription by hypoxia-inducible factor 1. Mol Cell Biol 1996;16:4604–13.
5. Mukhopadhyay D, Knebelmann B, Cohen HT, Ananth S, Sukhatme VP. The von Hippel-Lindau tumor suppressor gene product interacts with Sp1 to repress vascular endothelial growth factor promoter activity. Mol Cell Biol 1997;17:5629–39.
6. Zhang L, Yu D, Hu M, et al. Wild-type p53 suppresses angiogenesis in human leiomyosarcoma and synovial sarcoma by transcriptional suppression of vascular endothelial growth factor expression. Cancer Res 2000; 60:3655–61.
7. Rak J, Mitsuhashi Y, Bayko L, et al. Mutant ras oncogenes upregulate VEGF/VPF expression: implications for induction and inhibition of tumor angiogenesis. Cancer Res 1995;55:4575–80.
8. Weidner N, Folkman J, Pozza F, et al. Tumor angiogenesis: a new significant and independent prognostic indicator in early-stage breast carcinoma. J Natl Cancer Inst 1992;84:1875–87.
9. Toi M, Matsumoto T, Bando H. Vascular endothelial growth factor: its prognostic, predictive, and therapeutic implications. Lancet Oncol 2001;2: 667–73.
10. Hasan J, Byers R, Jayson GC. Intra-tumoural microvessel density in human solid tumours. Br J Cancer 2002;86:1566–77.
11. Keck PJ, Hauser SD, Krivi G, et al. Vascular permeability factor, an endothelial cell mitogen related to PDGF. Science 1989;246:1309–12.
12. Pepper MS, Ferrara N, Orci L, Montesano R. Potent synergism between vascular endothelial growth factor and basic fibroblast growth factor in the induction of angiogenesis *in vitro*. Biochem Biophys Res Commun 1992;189:824–31.
13. Goto F, Goto K, Weindel K, Folkman J. Synergistic effects of vascular endothelial growth factor and basic fibroblast growth factor on the proliferation and cord formation of bovine capillary endothelial cells within collagen gels. Lab Invest 1993;69:508–17.
14. Alon T, Hemo I, Itin A, Pe'er J, Stone J, Keshet E. Vascular endothelial growth factor acts as a survival factor for newly formed retinal vessels and has implications for retinopathy of prematurity. Nat Med 1995;1:1024–8.
15. Benjamin LE, Keshet E. Conditional switching of vascular endothelial growth factor (VEGF) expression in tumors: induction of endothelial cell shedding and regression of hemangioblastoma-like vessels by VEGF withdrawal. Proc Natl Acad Sci U S A 1997;94:8761–6.
16. Benjamin LE, Golijanin D, Itin A, Pode D, Keshet E. Selective ablation of immature blood vessels in established human tumors follows vascular endothelial growth factor withdrawal. J Clin Invest 1999;103:159–65.
17. Asahara T, Murohara T, Sullivan A, et al. Isolation of putative progenitor endothelial cells for angiogenesis. Science 1997;275:964–7.
18. Gehling UM, Ergun S, Schumacher U, et al. *In vitro* differentiation of endothelial cells from AC133-positive progenitor cells. Blood 2000;95: 3106–12.

Downloaded from mct.aacrjournals.org on April 10, 2021. © 2004 American Association for Cancer Research.

19. Neufeld G, Cohen T, Gengrinovitch S, Poltorak Z. Vascular endothelial growth factor (VEGF) and its receptors. FASEB J 1999;13:9 – 22.

20. Veikkola T, Karkkainen M, Claesson-Welsh L, Alitalo K. Regulation of angiogenesis via vascular endothelial growth factor receptors. Cancer Res 2000;60:203 – 12.

21. Takahashi T, Yamaguchi S, Chida K, Shibuya M. A single autophosphorylation site on KDR/Flk-1 is essential for VEGF-A-dependent activation of PLC- and DNA synthesis in vascular endothelial cells. EMBO J 2001; 20:2768 – 78.

22. Sawano A, Takahashi T, Yamaguchi S, Aonuma M, Shibuya M. Flt-1 but not KDR/Flk-1 tyrosine kinase is a receptor for placenta growth factor, which is related to vascular endothelial growth factor. Cell Growth Differ 1996;7:213 – 21.

23. Soker S, Gollamudi-Payne S, Fidder H, Charmahelli H, Klagsbrun M. Inhibition of vascular endothelial growth factor (VEGF)-induced endothelial cell proliferation by a peptide corresponding to the exon 7-encoded domain of VEGF165. J Biol Chem 1997;272:31582 – 8.

24. Roberts WG, Hasan T. Tumor-secreted vascular permeability factor/vascular endothelial growth factor influences photosensitizer uptake. Cancer Res 1993;53:153 – 7.

25. Wu LW, Mayo LD, Dunbar JD, et al. Utilization of distinct signaling pathways by receptors for vascular endothelial cell growth factor and other mitogens in the induction of endothelial cell proliferation. J Biol Chem 2000;275:5096 – 103.

26. McMahon G. VEGF receptor signaling in tumor angiogenesis. Oncologist 2000;5:3 – 10.

27. Glade-Bender J, Kandel JJ, Yamashiro DJ. VEGF blocking therapy in the treatment of cancer. Expert Opin Biol Ther 2003;3:263 – 76.

28. Ferrara N, Hillan KJ, Gerber HP, Novotny W. Discovery and development of bevacizumab, an anti-VEGF antibody for treating cancer. Nat Rev Drug Discov 2004;3:391 – 400.

29. Wood JM, Bold G, Buchdunger E, et al. PTK787/ZK 222584, a novel and potent inhibitor of vascular endothelial growth factor receptor tyrosine kinases, impairs vascular endothelial growth factor-induced responses and tumor growth after oral administration. Cancer Res 2000;60:2178 – 89.

30. Wedge SR, Ogilvie DJ, Dukes M, et al. ZD6474 inhibits vascular endothelial growth factor signaling, angiogenesis, and tumor growth following oral administration. Cancer Res 2002;62:4645 – 55.

31. Mendel DB, Laird AD, Xin X, et al. *In vivo* antitumor activity of SU11248, a novel tyrosine kinase inhibitor targeting vascular endothelial growth factor and platelet-derived growth factor receptors: determination of a pharmacokinetic/pharmacodynamic relationship. Clin Cancer Res 2003;9:327 – 37.

32. Ruggeri B, Singh J, Gingrich D, et al. CEP-7055: a novel, orally active pan inhibitor of vascular endothelial growth factor receptor tyrosine kinases with potent antiangiogenic activity and antitumor efficacy in preclinical models. Cancer Res 2003;63:5978 – 91.

33. Beebe JS, Jani JP, Knauth E, et al. Pharmacological characterization of CP-547,632, a novel vascular endothelial growth factor receptor-2 tyrosine kinase inhibitor for cancer therapy. Cancer Res 2003;63: 7301 – 9.

34. Sepp-Lorenzino L, Rands E, Mao X, et al. A novel orally bioavailable inhibitor of kinase insert domain-containing receptor induces antiangiogenic effects and prevents tumor growth *in vivo*. Cancer Res 2004;64: 751 – 6.

35. Ferrara N, Gerber HP, LeCouter J. The biology of VEGF and its receptors. Nat Med 2003;9:669 – 76.

36. Hiratsuka S, Minowa O, Kuno J, Noda T, Shibuya M. Flt-1 lacking the tyrosine kinase domain is sufficient for normal development and angiogenesis in mice. Proc Natl Acad Sci U S A 1998;95:9349 – 54.

37. Fong GH, Zhang L, Bryce DM, Peng J. Increased hemangioblast commitment, not vascular disorganization, is the primary defect in flt-1 knock-out mice. Development 1999;126:3015 – 25.

38. Salven P, Lymboussaki A, Heikkila P, et al. Vascular endothelial growth factors VEGF-B and VEGF-C are expressed in human tumors. Am J Pathol 1998;153:103 – 8.

39. Donnini S, Machein MR, Plate KH, Weich HA. Expression and localization of placenta growth factor and PlGF receptors in human meningiomas. J Pathol 1999;189:66 – 71.

40. Hiratsuka S, Maru Y, Okada A, Seiki M, Noda T, Shibuya M. Involvement of Flt-1 tyrosine kinase (vascular endothelial growth factor receptor-1) in pathological angiogenesis. Cancer Res 2001;61: 1207 – 13.

41. Carmeliet P, Moons L, Luttun A, et al. Synergism between vascular endothelial growth factor and placental growth factor contributes to angiogenesis and plasma extravasation in pathological conditions. Nat Med 2001;7:575 – 83.

42. Autiero M, Waltenberger J, Communi D, et al. Role of PlGF in the intra- and intermolecular cross talk between the VEGF receptors Flt1 and Flk1. Nat Med 2003;9:936 – 43.

43. Barleon B, Sozzani S, Zhou D, Weich HA, Mantovani A, Marme D. Migration of human monocytes in response to vascular endothelial growth factor (VEGF) is mediated via the VEGF receptor flt-1. Blood 1996;87: 3336 – 43.

44. Clauss M, Weich H, Breier G, et al. The vascular endothelial growth factor receptor Flt-1 mediates biological activities. Implications for a functional role of placenta growth factor in monocyte activation and chemotaxis. J Biol Chem 1996;271:17629 – 34.

45. Ono M, Torisu H, Fukushi J, Nishie A, Kuwano M. Biological implications of macrophage infiltration in human tumor angiogenesis. Cancer Chemother Pharmacol 1999;43:S69 – 71.

46. Kaipainen A, Korhonen J, Mustonen T, et al. Expression of the fms-like tyrosine kinase 4 gene becomes restricted to lymphatic endothelium during development. Proc Natl Acad Sci U S A 1995;92:3566 – 70.

47. Valtola R, Salven P, Heikkila P, et al. VEGFR-3 and its ligand VEGF-C are associated with angiogenesis in breast cancer. Am J Pathol 1999;154: 1381 – 90.

48. Pepper MS. Lymphangiogenesis and tumor metastasis: myth or reality? Clin Cancer Res 2001;7:462 – 8.

49. Murohara T, Horowitz JR, Silver M, et al. Vascular endothelial growth factor/vascular permeability factor enhances vascular permeability via nitric oxide and prostacyclin. Circulation 1998;97:99 – 107.

50. Dvorak HF, Brown LF, Detmar M, Dvorak AM. Vascular permeability factor/vascular endothelial growth factor, microvascular hyperpermeability, and angiogenesis. Am J Pathol 1995;146:1029 – 39.

Downloaded from mct.aacrjournals.org on April 10, 2021. © 2004 American Association for Cancer Research.

AACR American Association for Cancer Research

Molecular Cancer Therapeutics

KRN633: A selective inhibitor of vascular endothelial growth factor receptor-2 tyrosine kinase that suppresses tumor angiogenesis and growth

Kazuhide Nakamura, Atsushi Yamamoto, Masaru Kamishohara, et al.

Mol Cancer Ther 2004;3:1639-1649.

Updated version Access the most recent version of this article at:
http://mct.aacrjournals.org/content/3/12/1639

Cited articles This article cites 46 articles, 27 of which you can access for free at:
http://mct.aacrjournals.org/content/3/12/1639.full#ref-list-1

Citing articles This article has been cited by 11 HighWire-hosted articles. Access the articles at:
http://mct.aacrjournals.org/content/3/12/1639.full#related-urls

E-mail alerts Sign up to receive free email-alerts related to this article or journal.

Reprints and Subscriptions To order reprints of this article or to subscribe to the journal, contact the AACR Publications Department at pubs@aacr.org.

Permissions To request permission to re-use all or part of this article, use this link
http://mct.aacrjournals.org/content/3/12/1639.
Click on "Request Permissions" which will take you to the Copyright Clearance Center's (CCC)
Rightslink site.

Downloaded from mct.aacrjournals.org on April 10, 2021. © 2004 American Association for Cancer Research.